

Strength characterisation of soil-based construction materials

C.T.S. Beckett^a, C.E. Augarde^b, D. Easton^c, T. Easton^c

^a*School of Civil, Environmental and Mining Engineering, University of Western Australia, Perth, WA 6009*

^b*School of Engineering and Computing Sciences, Durham University, Durham, DH1 3LE, UK*

^c*Watershed Materials, 11 Basalt Road, Napa, CA 94558, USA*

Abstract

Rammed earth (RE) is a venerable construction technique, gaining attention today due to its environmental and sustainable qualities. A key obstacle to its wider adoption is a lack of strength characterisation methods to aid in design and conservation. Research over the past decade has demonstrated that suction is the key mechanism behind strength and strength gain. As suction changes with the building's environment, being able to predict strength changes with suction is essential for practitioners and conservators alike. This paper presents a method for predicting RE strengths based on the Extended Mohr Coulomb (EMC) framework. Construction of an EMC failure envelope in the residual suction range is discussed and the use of a planar envelope justified. Unconfined compression and indirect tensile tests on two RE soils are used to construct this envelope and methods to predict strengths from it are derived. Excellent agreement between measured and predicted strengths is also found for available literature data. Simplifications are identified to adapt the developed technique to suit RE practice and a suitable experimental procedure is outlined. Finally, the revised experimental procedure is employed at an existing RE construction facility to successfully predict strengths of a compacted Californian sandy loam.

Keywords: Rammed earth, suction, Extended Mohr-Coulomb, climate change

1 1. Introduction

2 Although the ancient practice of rammed earth (RE) has been demonstrably
3 successful for millennia, the global renaissance of this venerable technique, which
4 is currently underway across the globe, has been hampered by the imposition of
5 engineering standards that are more appropriate to reinforced concrete. In order
6 to secure building code compliance, RE practitioners find themselves required
7 to attain compressive strengths for their installed wall systems (e.g. NZS 4297,
8 Walker and Standards Australia (2002)) that are usually beyond those achievable
9 for soil-based masonry unless Portland cement or other CO₂ generating stabilizers
10 are used to augment the clay-based aggregates.

11 Clearly, history demonstrates durability for RE that contradicts the strength
12 requirements currently mandated. The RE industry, albeit a small fraction of
13 the more conventional cement-based masonry industry, can benefit from a set of
14 testing protocols that will establish a new set of limits (or standards) from which
15 the testing and permitting agencies can align with the practitioners. Given that
16 unstabilised RE is far more susceptible to strength loss at saturation than sta-
17 bilized rammed earth, a thorough understanding of the mechanisms that govern
18 strength gain and strength loss in clay-based aggregates is critical to the ultimate
19 success of the industry. Concurrently, RE and other earthen buildings represent
20 a significant proportion of our built heritage. Maintaining this heritage demands
21 a scientific approach to predict and forecast material properties. Therefore, this

Email addresses: christopher.beckett@uwa.edu.au (C.T.S. Beckett),
charles.augarde@dur.ac.uk (C.E. Augarde), david@watershedmaterials.com (D. Easton),
taj@watershedmaterials.com (T. Easton)

22 paper sets out to: i) experimentally examine RE strength variation through a
23 comprehensive experimental campaign; ii) develop a framework to predict RE
24 strength change given known environmental conditions; iii) adapt that frame-
25 work to devise a series of characterisation tests sufficiently simple to be useful for
26 practice.

27 **2. Experimental programme**

28 Suction is a key factor responsible for developing RE's strength and the source
29 of its ability to maintain, in effect, vertical 'slopes' for thousands of years. Un-
30 derstanding the effects of suction variation is therefore critical to any attempt to
31 characterise RE behaviour (Jaquin et al., 2009; Gerard et al., 2015). This sec-
32 tion describes the experimental programme developed to investigate RE strength
33 under controlled suction conditions.

34 *2.1. Materials*

35 Site soils can be highly variable and so are inconvenient for laboratory inves-
36 tigations. Instead, 'engineered' soils, manufactured from known quantities of raw
37 materials, were used in this study to guarantee mineralogical and grading con-
38 sistency. Soils used in this investigation were selected to represent the range of
39 materials used for RE construction around the world are listed in Table 1. Soils
40 were named after their targeted constituent proportions; for example, Soil 4-5-1
41 nominally comprised 40% silty clay ("Birtley" clay, LL 58.8%, PL 25.7%, 50%
42 kaolinitic clay), 50% sand and 10% gravel by mass. Soils 4-5-1 and 2-7-1 com-
43 prised the maximum and minimum recommended silty clay ($\leq 60\mu\text{m}$) contents for
44 RE materials respectively (Houben and Guillaud, 1996), to investigate behaviour
45 at the extreme material boundaries. Both soils had the minimum recommended

Table 1: Soil mix constituents, OWC and $\rho_{d,max}$

Soil	Clay (%)	Silt (%)	Sand (%)	Gravel (%)	OWC (%)	$\rho_{d,max}$ (kg/m ³)
4-5-1	19.9	17.2	52.7	10.2	12.0	1940
2-7-1	9.9	9.5	70.7	9.9	12.0	1960

46 gravel contents (10%) to reduce the influence of large particles on test results and
 47 are considered sandy loams by the USDA classification system. Grading curves
 48 are given in Figure 1. Soil optimum water contents (OWCs) and maximum dry
 49 densities ($\rho_{d,max}$) were determined using the Standard Proctor Test (BS 1377),
 50 also given in Table 1.

51 (Insert Figure 1 somewhere near here)

52 2.2. Strength testing

53 The Vapour Equilibrium (VE) method was used to control suction during
 54 testing by equilibrating specimens to set temperatures (T) and relative humidities
 55 (RH). Under equilibrium conditions, total suction, ψ_t , is controlled by T and RH
 56 according to the Kelvin Equation:

$$\psi_t = -\frac{R_u T}{v_m} \ln(\text{RH}) \quad (1)$$

57 where T is absolute temperature, R_u is the universal gas constant (8.314 J/molK)
 58 and v_m is the molar volume of pure water (18.016×10^{-6} m³/mol). Suction is
 59 highly sensitive to seemingly minor changes in atmospheric conditions; by Eqn 1,
 60 reducing RH from 70% to 50% at 20°C increases suction from 48.3 to 93.8 MPa.

61 Strengths at different suction values were examined using a combination of
 62 unconfined compression (UCS) and indirect tensile (ITS) testing. UCS is com-
 63 monly used to compare the performance of different RE soils and so is a technique

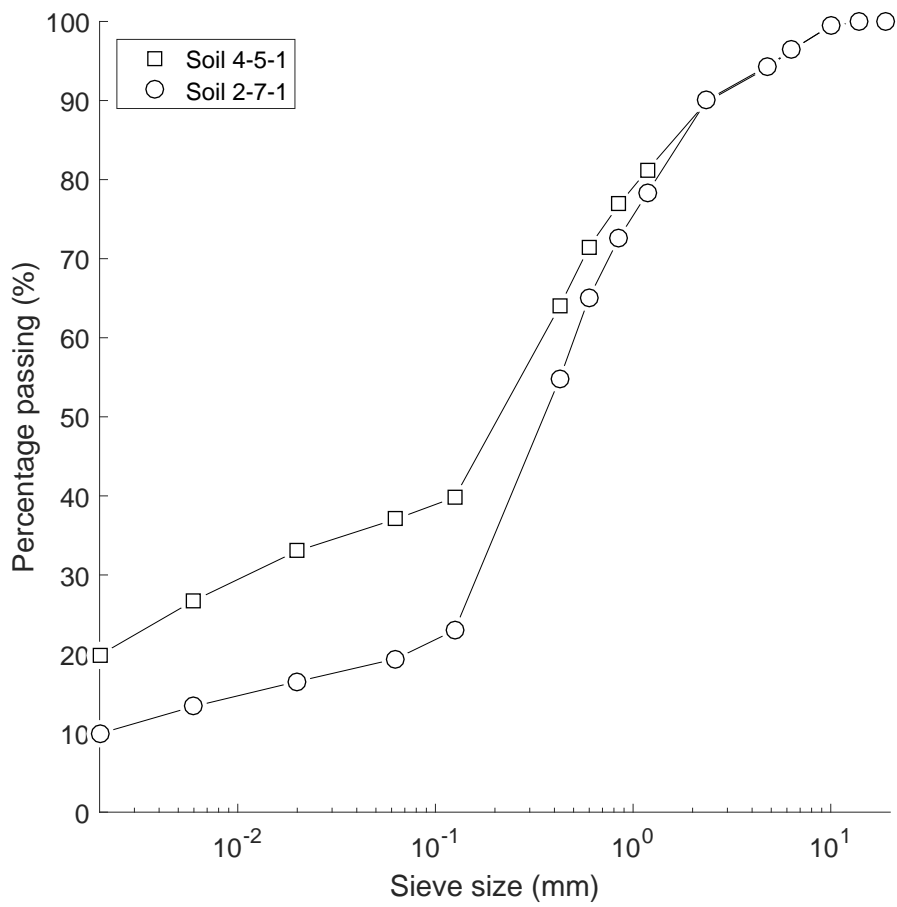


Figure 1: Particle grading curves for mixes 4-5-1 and 2-7-1

64 already familiar to RE practitioners. ITS was selected as specimen manufacture,
65 handling and testing procedures are similar to those used for UCS testing and
66 so can be accommodated by practitioners' existing facilities and expertise. ITS
67 testing was previously reported in Beckett et al. (2015) but is briefly discussed
68 here for convenience.

69 2.2.1. UCS testing

70 100mm cube specimens were manufactured for UCS testing. Although it is
71 common to use $\varnothing 100 \times 200$ mm cylindrical specimens, the smaller cube specimens
72 were selected to reduce the amount of material needed. UCS specimens were
73 manufactured at the OWC (using deionised water) and to $\rho_{d,max}$ for that mix
74 (Table 1) by compacting three equal layers of known mass to a controlled vol-
75 ume. The upper surface of the specimen was scraped and depressions filled with
76 a screed of fine material (parent soil sieved to pass 0.450mm) to ensure a level
77 surface; this was necessary as specimens could not be rotated to present level
78 surfaces, as is done when testing concrete. Specimens were removed from the
79 mould immediately following manufacture and left to dry on wire racks under
80 conditions of $20 \pm 2^\circ\text{C}$ and $45 \pm 15\%$ RH until reaching a constant mass for two
81 consecutive days. Specimens were then equilibrated to RH=30, 50, 70 or 90%
82 ($\pm 3\%$) and $T = 15, 20, 30$ or 40°C ($\pm 2^\circ\text{C}$) (14–174MPa suction by Eqn 1) us-
83 ing an environmental chamber (EC, Vötsch VC4033). An initial drying period
84 was necessary prior to equilibration due to limited EC availability and difficul-
85 ties in transporting fresh specimens. Specimens therefore either gained or lost
86 water to achieve their final equilibration: consequences of testing specimens un-
87 der wetting or drying conditions are discussed in the following sections. Once
88 equilibrated, specimens were immediately transferred to a testing machine and

89 uniaxially loaded at a controlled displacement rate of 0.5mm/min until failure.
90 Specimens were not capped as surfaces were level. Specimen water contents were
91 determined by oven drying crushed material. Three specimens were manufac-
92 tured per RH and T combination per soil; 96 in total.

93 RH and T values were selected to be representative of typical atmospheric
94 conditions at RE sites around the world (Beckett and Augarde, 2012). How-
95 ever, moisture contents can also be affected by incident rainfall or capillary rise
96 (Hall and Djerbib, 2004). Under such circumstances, suction values are likely
97 to fall below those examined here. However, these events constitute failures of
98 the structural design, so that material would not be exposed to such conditions
99 under normal circumstances. Consequences of suctions falling significantly below
100 examined levels are discussed in the following sections. It should also be noted
101 that UCS specimens behaved as soil elements due to equilibration to constant
102 suction conditions. In practice, water content gradients may exist through RE
103 structural components due to hygrothermal interactions with the surrounding
104 atmosphere (McGregor et al., 2015). As such, our testing programme was not
105 representative of *structural* element behaviour but can be used to assess potential
106 strength changes along a moisture or suction gradient.

107 2.2.2. ITS testing

108 $\varnothing 100 \times 50$ mm ‘disc’ specimens were manufactured following a similar proce-
109 dure to that for UCS specimens. Specimens were removed from the mould and
110 air-dried on wire racks to a target water content, then wrapped in clear plastic
111 for a minimum of two days for suction equilibration. Specimens were tested to
112 failure at a displacement rate of 0.2mm/min between curved metal platens. Man-
113 ufacturing and orientating specimens in this way tested indirect tensile strength

114 perpendicular to the compaction planes (Beckett et al., 2015). Tensile strength,
115 σ_t , was determined via

$$\sigma_t = -\frac{P}{\pi RL} \quad (2)$$

116 where P is the applied compressive load and R and L are the specimen radius
117 and length respectively. Eqn 2 is valid for specimens with little deformation
118 (Frydman, 1964). The highest suctions achieved from air-drying ITS specimens
119 were 60 and 80 MPa for Soils 4-5-1 and 2-7-1 respectively. The minimum suction
120 was roughly 1 MPa for both soils. Again, ITS testing was representative of soil,
121 rather than structural, elements.

122 *2.3. Soil water retention properties*

123 Soil-water retention properties for Soils 4-5-1 and 2-7-1 were reported in Beck-
124 ett et al. (2015). For convenience, the procedures used are briefly discussed here.
125 Drying retention properties were determined using a combination of filter paper
126 (suctions 0 to 4 MPa) and vapour-equilibrium (10 to 200 MPa) methods. Filter
127 paper testing followed ASTM D5298-10. The relationship

$$\ln \psi_t = -4.6234 - 3.6454 \ln(w_{fp}) \quad (3)$$

128 was used to calculate ψ_t from the gravimetric water contents (w_{fp}) of suspended
129 filter papers (i.e. those in equilibrium with the surrounding air), determined via
130 a best-fit relationship to data presented in Hamblin (1981). Soil water retention

131 curves (SWRCs) for each mix are shown in Figure 2, where data were fitted using

$$C = \left(1 + \frac{\log\left(1 + \frac{\psi_t}{10^9}\right)}{\log(2)} \right) \quad (4)$$

$$S_r = C \times \frac{1}{\left(\ln\left(\epsilon + \left(\frac{\psi_t}{a}\right)^n\right)\right)^m} \quad (5)$$

132 where S_r is the degree of saturation, ϵ is the Euler number, C is a correction term
133 limiting S_r to 0 at $\psi_t = 1\text{GPa}$ and a , m and n are fitting parameters given in
134 Figure 2 (Fredlund and Xing, 1994). Residual suction values (ψ_{res}) were found
135 from intersecting lines drawn tangentially to the steepest and shallowest parts
136 of the curve. Although it is common to impose that the latter tangent passes
137 through $S_r = 0$ at $\psi_t = 1\text{GPa}$, the correction term in Eqn 5 causes bimodality
138 in the high suction portion of the SWRC, producing an unrealistic estimation of
139 ψ_{res} ; tangents to the shallowest section of the curve were therefore used. ψ_{res}
140 and $S_{r,res}$ are given in Figure 2.

141 (Insert Figure 2 somewhere near here)

142 3. Experimental results

143 UCS values for Soils 4-5-1 and 2-7-1 are shown in Figures 3 and 4 respectively.
144 Note that UCS was not factored to account for the use of cubic, rather than the
145 more common cylindrical, specimens. ITS results for untreated Soils 4-5-1 and
146 2-7-1 from Beckett et al. (2015) are shown in Figure 5.

147 Figures 3 to 5 show that UCS roughly doubled and ITS increased tenfold
148 between the lowest and highest tested suction conditions for both soils. It is
149 possible that an RE structure might experience the full range of these conditions
150 over the course of a single year; given their large surface area, equilibration to such

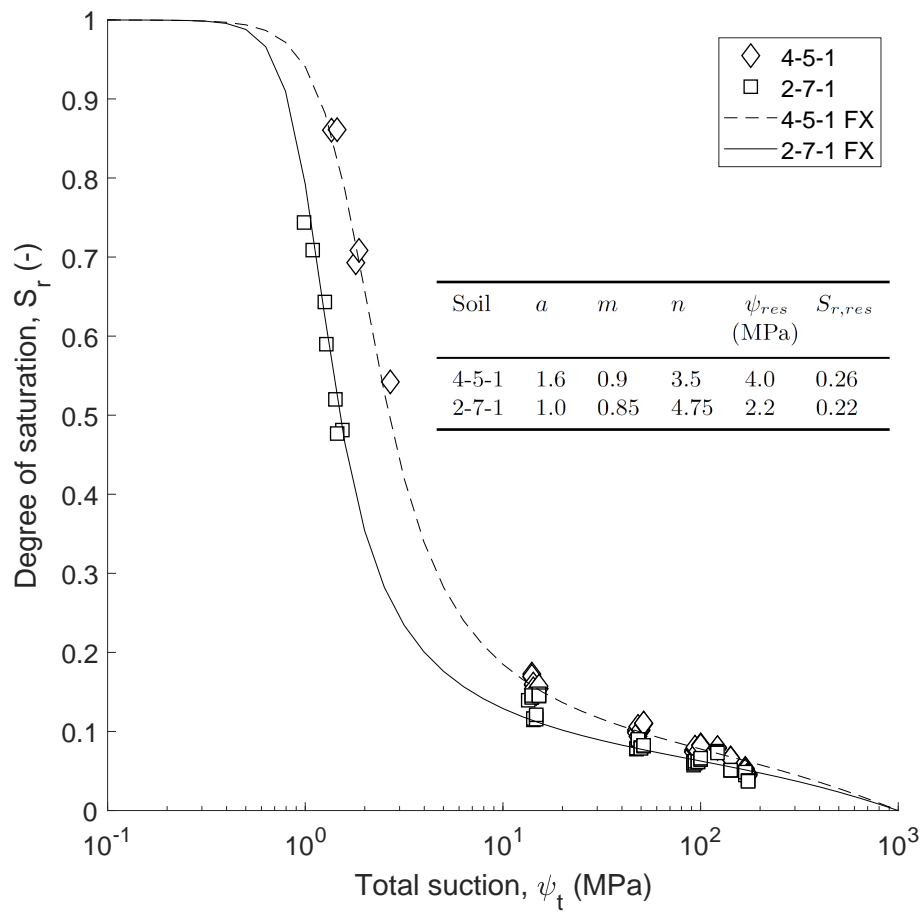


Figure 2: Soil 4-5-1 and 2-7-1 drying retention curves and fitting parameters. FX: fit using Eqn 5

151 conditions is rapid and large changes in strength over a building's life may result.
152 Suction variation must therefore form the basis of any strength characterisation
153 methods. The development of such a method is discussed in the following sections.

154 (Insert Figure 3 somewhere near here)

155 (Insert Figure 4 somewhere near here)

156 (Insert Figure 5 somewhere near here)

157 4. Constitutive model development

158 4.1. Extended Mohr-Coulomb failure criterion in the residual suction range

159 Two common approaches exist to incorporate suction into an effective stress
160 framework. The generalised effective stress method uses an effective stress pa-
161 rameter, χ , to modify the existing pore water pressure term:

$$\sigma' = \sigma - \chi(u_a - u_w) \quad (6)$$

162 where u_a and u_w are the pore air and water pressures respectively. The advantage
163 of Eqn 6 is that it is similar in construction to the Terzaghi effective stress
164 approach familiar to most geotechnical engineers. However, the form of χ is
165 disputed and heavily dependent on the form of the SWRC (Khalili and Khabbaz,
166 1998). An alternative to this approach is to introduce suction as a third stress
167 state variable (Fredlund and Morgenstern, 1977). Shear strength is calculated
168 via

$$\tau_f = c' + (\sigma - u_a) \tan \phi' + (u_a - u_w) \tan \phi^b \quad (7)$$

169 where c' is the effective cohesion, ϕ' is the effective friction angle associated with
170 net stress and $\tan \phi^b$ is the friction angle associated with a change in suction

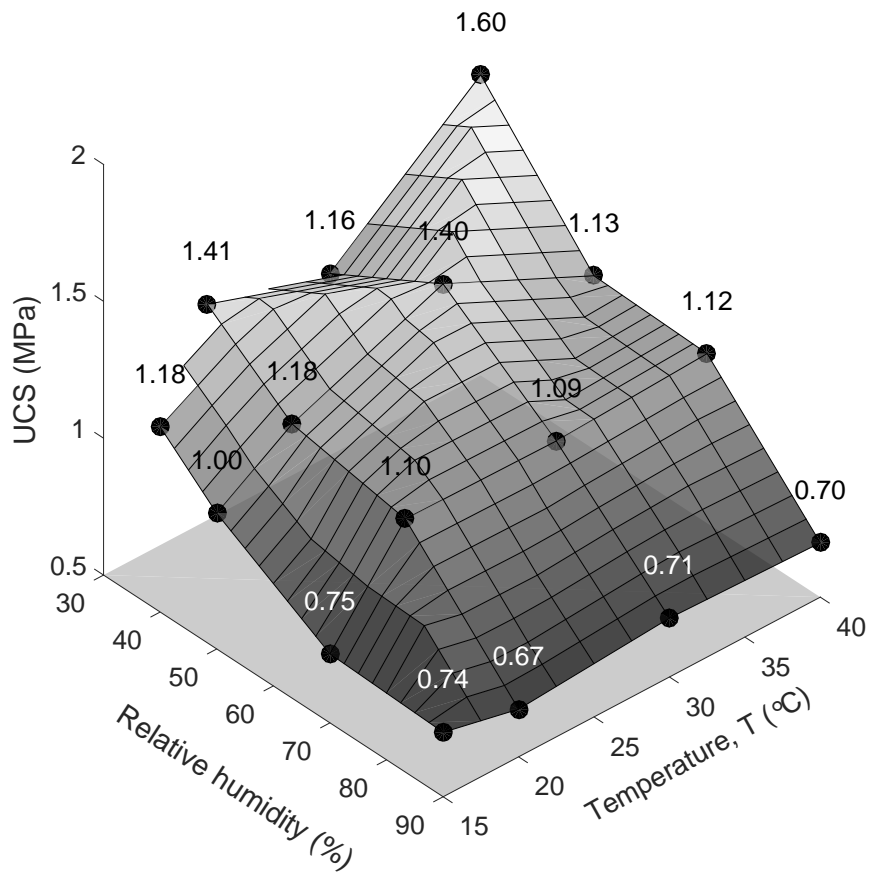


Figure 3: UCS results for Soil 4-5-1 (individual values shown above markers)

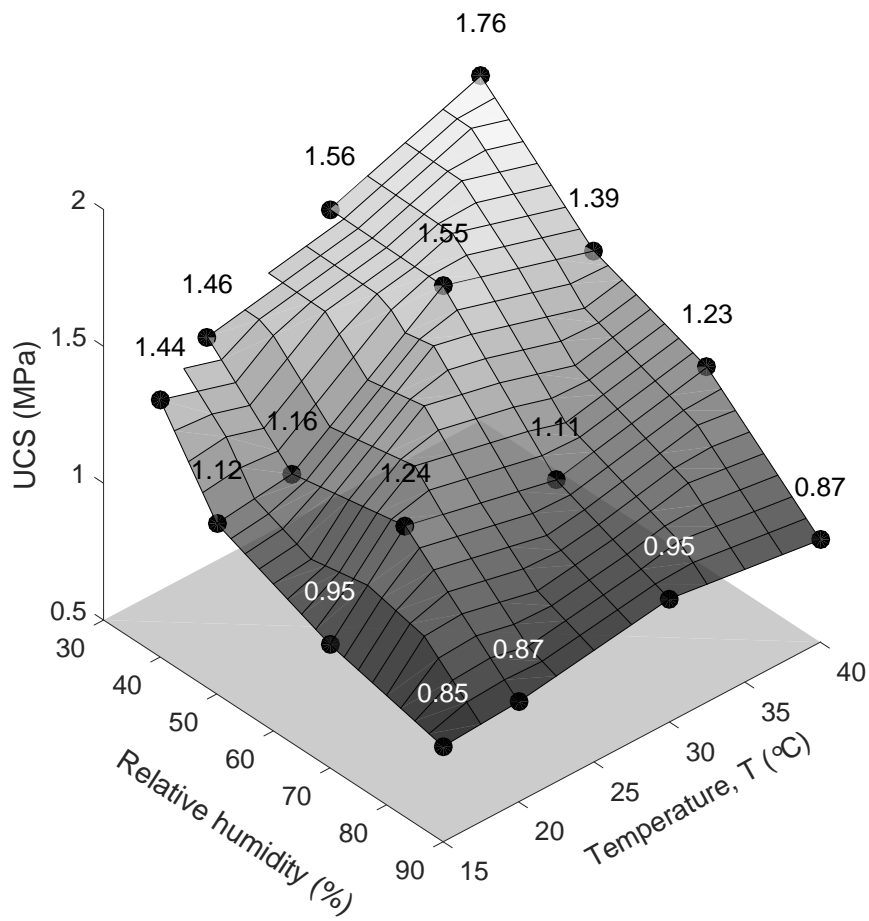


Figure 4: UCS results for Soil 2-7-1 (individual values shown above markers)

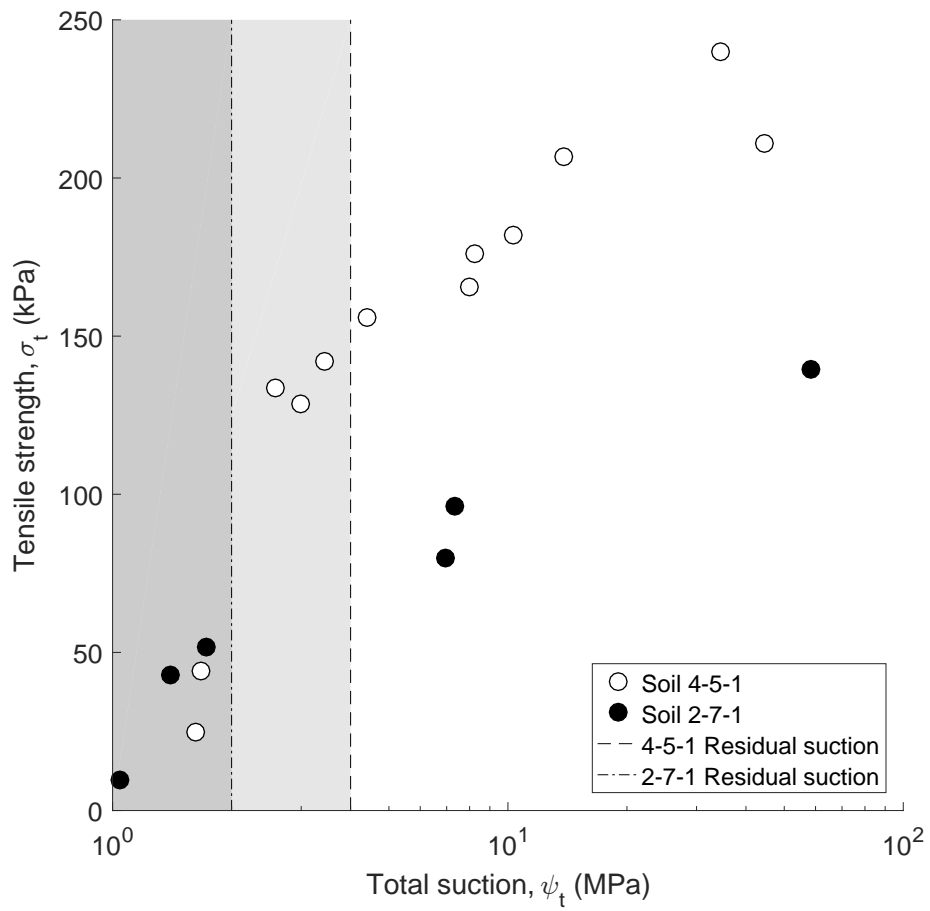


Figure 5: ITS results for Soils 4-5-1 and 2-7-1 from Beckett et al. (2015). Shaded regions show suctions below residual values

171 a constant value of net stress ($\sigma - u_a$). It is generally accepted that ϕ^b is a
 172 function of S_r and diminishes to small values as S_r approaches zero (Gan et al.,
 173 1988; Fredlund and Rahardjo, 1993). The advantage of this “extended” Mohr-
 174 Coulomb criterion (EMC) is that the contributions of suction and net stress can
 175 be assessed separately.

176 ϕ' is commonly assumed to be constant in the residual suction range (Fredlund
 177 et al., 1987). However, the form of ϕ^b depends on the range of suction investi-
 178 gated. Fredlund et al. (1996) and Vanapalli et al. (1996) presented a method to
 179 predict values of ϕ^b from ϕ' for given values of suction, via

$$\tan \phi^b = \left(\Theta(\psi)^\kappa + \psi \frac{d(\Theta(\psi)^\kappa)}{d\psi} \right) \tan \phi' \quad (8)$$

180 where $\Theta = \frac{\theta(\psi) - \theta_{res}}{\theta_s - \theta_{res}}$, $\theta(\psi)$, θ_s and θ_{res} are the volumetric water contents at
 181 the current, saturation and residual suction values respectively and κ is a fitting
 182 parameter. Note that, for brevity, ψ_t has been contracted to ψ in all equations
 183 from Eqn 8 onwards. As $\Theta \leq 1 \forall \psi$, Eqn 8 maintains $\phi^b < \phi'$ for suctions above
 184 the air-entry value as discussed above. To avoid negative values of Θ for $\theta < \theta_{res}$,
 185 Eqn 8 can be simplified by assuming $\theta_{res} = 0$ so that $\Theta = S_r$, i.e.

$$\tan \phi^b = \left(S_r(\psi)^\kappa + \psi \frac{d(S_r(\psi)^\kappa)}{d\psi} \right) \tan \phi'. \quad (9)$$

186 Depending on the expression used for the SWRC (e.g. Eqn 5), $\frac{d(S_r^\kappa)}{d\psi}$ in Eqn 9 can
 187 be quite involved. However, assuming a linear SWRC in the residual suction range
 188 (as supported by Figure 2) reduces $\frac{d(S_r(\psi)^\kappa)}{d\psi}$ to a constant value. As $\frac{d(S_r(\psi)^\kappa)}{d\psi}$ is
 189 small, $S_r(\psi)^\kappa$ is also nominally constant. Therefore, in the residual suction range,
 190 we assumed ϕ^b to be constant and so the failure envelope to be planar.

Table 2: EMC parameters determined for RE soils

Soil	c' (MPa)	ϕ' ($^\circ$)	ϕ^b ($^\circ$)	ϕ^b ($^\circ$, Eqn 9)	κ (Eqn 9)	Fitted suction range (MPa)
4-5-1	0.24	24.5	0.082	0.084	1.25	4.0–60
2-7-1	0.15	39.7	0.093	0.092	1.44	4.0–80

191 *4.2. Modelling experimental data*

192 UCS data discussed above and ITS results for untreated material from Beckett
 193 et al. (2015) were used to construct EMC failure surfaces for Soils 4-5-1 and
 194 2-7-1. Construction of the failure envelope from UCS and ITS data is shown
 195 schematically in Figure 6. The final fitted plane for 2-7-1 is shown in Figure 7.
 196 Mohr’s circles for UCS tests were drawn assuming that $\sigma_2 = \sigma_3 = 0$ and $\sigma_1 = \sigma_c$.
 197 ITS Mohr’s circles were drawn assuming $\sigma_2 = 0$, $\sigma_3 = \sigma_t$ and $\sigma_1 = -3\sigma_t$ (noting
 198 that σ_t is negative in Eqn 2). ITS relationships were derived in Li and Wong
 199 (2013) and are valid for specimens with little deformation, as is the case for such
 200 high suction values. Circles were discretised and points for best plane fitting were
 201 determined via a least squares approach. Planes were fitted using the suction
 202 range for which both UCS and ITS data were available. c' , ϕ' and ϕ^b and the
 203 fitted suction range for each soil are given in Table 2.

204 (Insert Figure 6 somewhere near here)

205 ϕ' values in Table 2 were similar to those typically found for compacted sandy
 206 loam soils, e.g. Vanapalli et al. (1996). Although ϕ^b values were close to zero,
 207 as expected for results in the residual suction range, the contribution of ϕ^b to
 208 strength was significant due to the high values of suction present. κ was selected
 209 to produce the best match between experimental ϕ^b values and those found via
 210 Eqn 9 using experimentally-derived ϕ' and SWRCs. κ fell within the $\kappa = 1-3$ lim-
 211 its suggested by Fredlund et al. (1996) for both soils, supporting the assumption

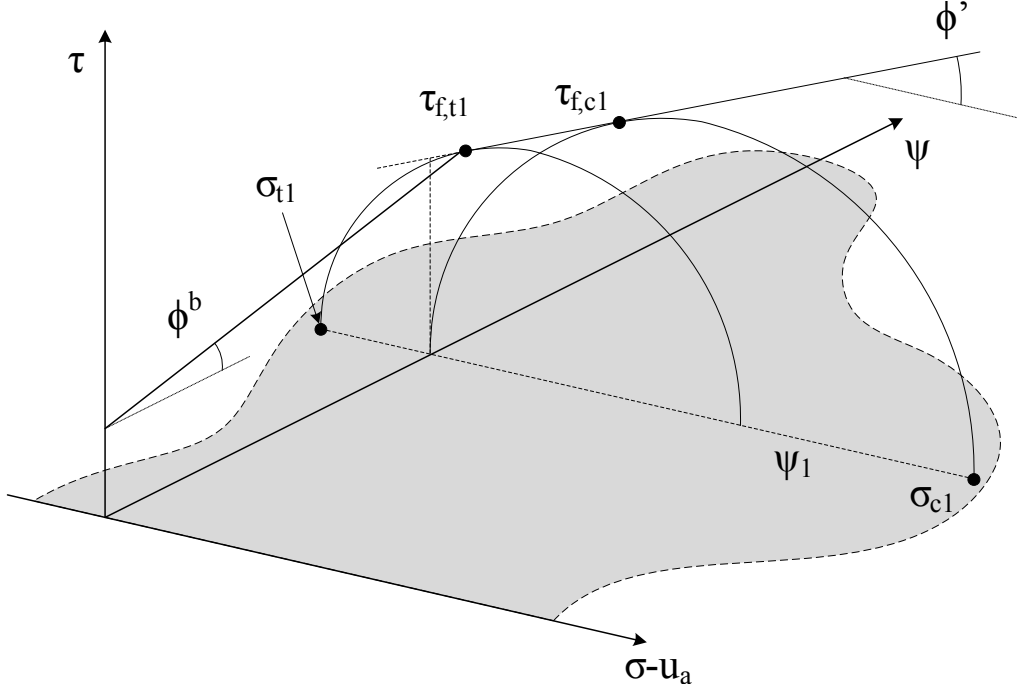


Figure 6: Construction of the planar EMC failure envelope using UCS and ITS data

212 of a planar failure envelope in the residual suction range. Although Soil 2-7-1
 213 achieved a higher UCS for all tested suction values, the fitted plane had a lower
 214 c' value than for Soil 4-5-1; this was due to the poor performance of Soil 2-7-1
 215 in tension. Soil 2-7-1's lower c' was countered by higher ϕ' and ϕ^b values. A
 216 higher ϕ' value was likely due to Soil 2-7-1's higher dry density and so greater
 217 particle interlock. The higher ϕ^b value was due to a shallower retention curve
 218 in the residual range, diminishing the contribution of the term in parentheses
 219 (negative) in Eqn 9.

220 (Insert Figure 7 somewhere near here)

221 UCS can be predicted from fitted c' , ϕ' and ϕ^b values via

$$\text{UCS} = 2 \left(\frac{c' + \psi \tan \phi^b}{\cos \phi' - (1 - \sin \phi') \tan \phi'} \right) \quad (10)$$

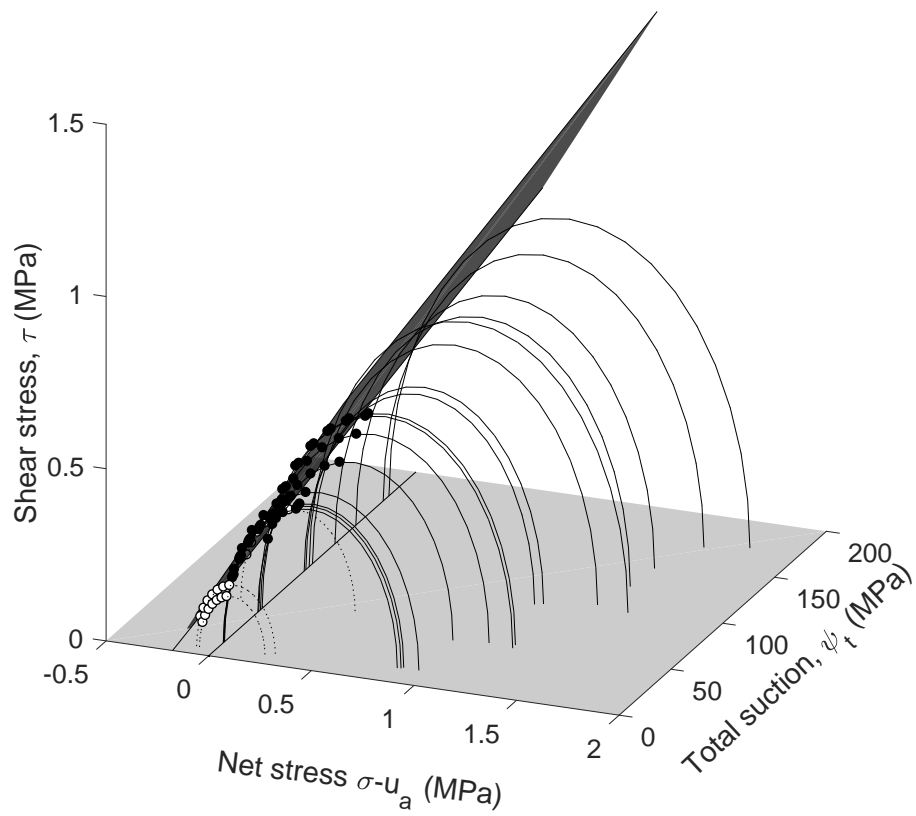


Figure 7: Soil 2-7-1 planar EMC failure envelope. - UCS results; - - ITS results. Markers denote points on the circles used for plane fitting. Mohr's circles without markers fell outside the ITS suction range

222 Eqn 10 is similar to that proposed by Panayiotopoulos (1996) to find UCS using
223 the generalised effective stress approach, however it maintains a clear distinc-
224 tion between the suction (the numerator) and internal friction (the denominator)
225 contributions to UCS. Figure 8 compares measured UCS values for mixes 4-5-1
226 and 2-7-1 and those predicted via Eqn 10. Predictions fall evenly about the line
227 of equality (± 0.15 MPa). Notably, there was no significant change in prediction
228 accuracy for UCS values above the upper ITS suction limit (i.e. above the range
229 for which plane fitting was defined) for either soil. Good accuracy beyond the fit-
230 ted range was due to the near-linear SWRC for suctions above the residual value.
231 Given the sensitivity of the SWRC gradient to the correction term in Eqn 5 in the
232 residual range, it is likely that the quality of fit would reduce for suctions much
233 higher than those tested. The fit quality would also suffer for suctions below the
234 residual value, for example as might arise during capillary rise. However, for the
235 range investigated, a planar failure envelope was suitable.

236 (Insert Figure 8 somewhere near here)

237 4.3. Application to literature data

238 Few suction-dependent RE strength datasets are available in the literature.
239 However, RE water retention and UCS data were presented in Jaquin et al.
240 (2009), Bui et al. (2014) and Gerard et al. (2015). Properties of those soils are
241 given in Table 9. Failure planes were fitted to Mohr's circles in the residual suction
242 range, as judged by SWRCs in those works, using the procedures discussed in the
243 previous section. As only UCS data was available for data in Jaquin et al. (2009)
244 and Bui et al. (2014), plane fitting was forcibly restricted to $\phi', \phi^b > 0$. The
245 full procedure was implemented for data from Gerard et al. (2015). c', ϕ' and ϕ^b
246 values for these soils are given in Table 4 and measured and predicted UCS values

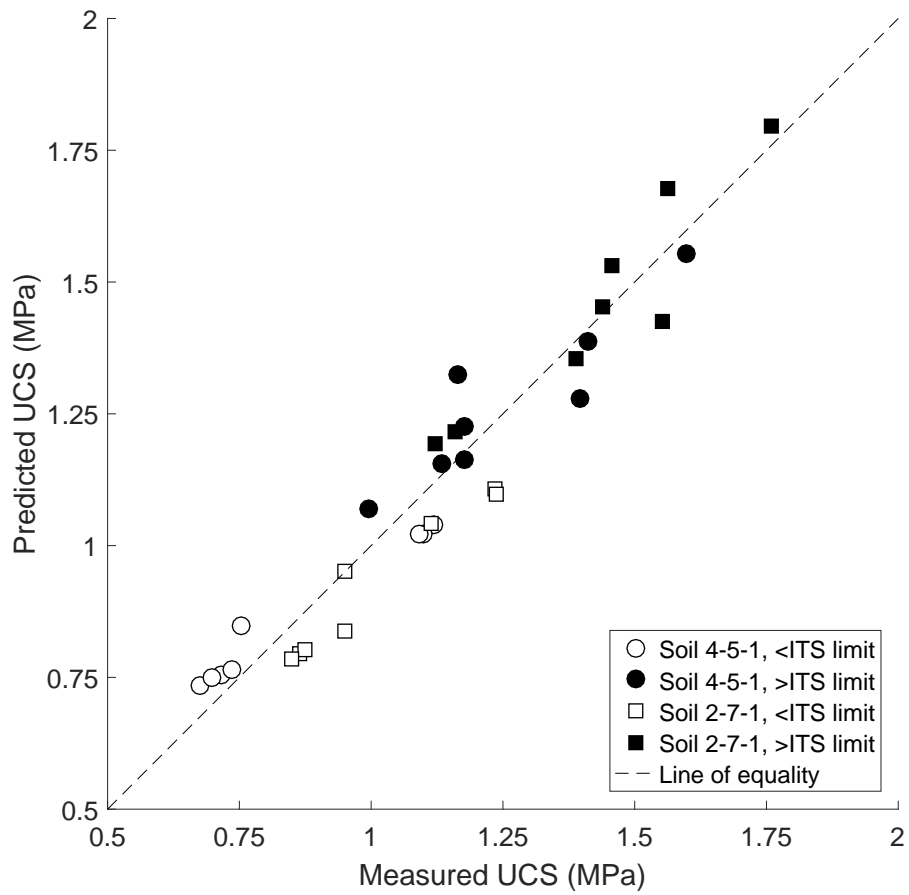


Figure 8: Comparison of measured and predicted UCS above and below ITS suction limit

Table 3: Constituents of soils used in the literature. CWC: Compaction Water Content. *Stabilised with 2% natural hydraulic lime. **Predominantly kaolinitic. ***Predominantly montmorillonitic

Soil	Clay (%)	Silt (%)	Sand (%)	Gravel (%)	CWC (%)	$\rho_{d,max}$ (kg/m ³)
Jaquin et al. (2009)	—15**—		25	60	12	2040
Bui et al. (2014) Soil A	5***	30	49	16	11	1920
Bui et al. (2014) Soil B*	4***	35	59	2	11	1920
Bui et al. (2014) Soil C	9***	38	50	3	11	1920
Gerard et al. (2015)	13**	64	26	0	15	1840

247 are compared in Figure 9. ϕ^b values were larger than those in Table 2 due to the
248 narrower fitted suction range. Excepting Bui et al. (2014) Soil C, κ values outside
249 of the 1–3 limit were required to match experimental and predicted ϕ^b values,
250 most notably for Jaquin et al. (2009). By Eqn 9, a low κ value indicated little
251 contribution of suction or saturation changes to changes in ϕ^b , so that $\phi^b \approx \phi'$
252 as is expected at low suction. That values marginally outside the 1–3 limit were
253 needed to fit other soils is reasonable given the restriction to UCS results only for
254 Bui et al. (2014) or the extremely high strengths found in Gerard et al. (2015).
255 Notably, the fit quality was seemingly unaffected the presence of stabiliser (Bui
256 et al. (2014) Soil B); this was perhaps to be expected, given the low stabiliser
257 and clay contents (for lime, the latter is required for the former to react) and the
258 strong contribution of suction to strength for weakly lime-stabilised RE (Ciancio
259 et al., 2014).

260 (Insert Figure 9 somewhere near here)

261 5. Adaptation to practice

262 At present, RE construction is hampered by a lack of construction codes or
263 standards and a shallow pool of available contractors. It is therefore unrealistic to
264 assume that RE practitioners can perform a wide range tests for every potential

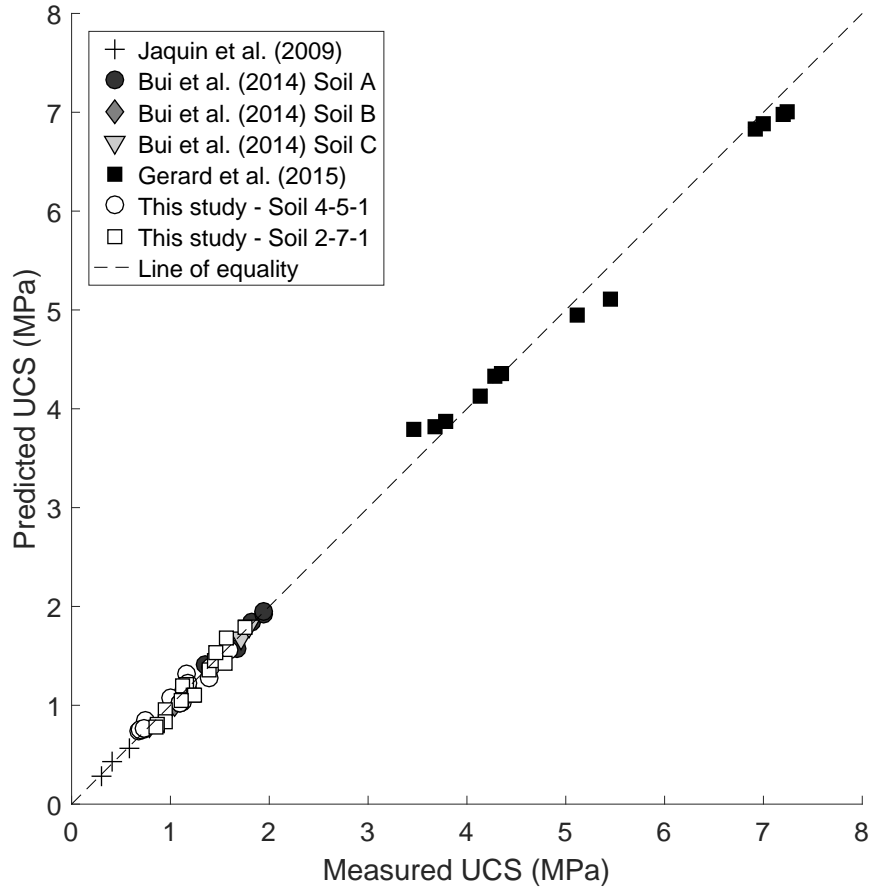


Figure 9: Measured and predicted UCS values for literature soil data

Table 4: EMC parameters derived for literature soils. *Matric suction, assumed to be total values for plane fitting

Soil	c' (kPa)	ϕ' ($^\circ$)	ϕ^b ($^\circ$)	ϕ^b ($^\circ$, Eqn 9)	κ (Eqn 9)	Suction range (MPa)
Jaquin et al. (2009)	83.1	11.42	10.62	10.62	0.09	0.18–0.80*
Bui et al. (2014) Soil A	512.7	11.92	0.24	0.24	3.72	3.2–65
Bui et al. (2014) Soil B	267.7	11.34	1.03	1.04	0.93	3.2–11
Bui et al. (2014) Soil C	566.2	12.63	0.25	0.25	1.25	8.1–36
Gerard et al. (2015)	929.4	38.5	0.32	0.32	3.07	4.1–126

265 RE soil or can afford the cost and delay of a lengthy laboratory campaign. To be
266 useful to RE industry, the EMC method discussed above can be simplified in three
267 key areas: i) tangential plane selection; ii) plane fitting; iii) testing equipment.

268 5.1. Plane selection

269 A complex (and potentially subjective) step of the plane-fitting process is
270 identifying the most accurate tangent to the Mohr's circles. An alternative to
271 a tangential failure envelope is to draw the envelope passing through the circle
272 maxima, as shown in Figure 10 where subscripts c and t denote compression
273 and tension respectively (Fredlund and Rahardjo, 1993). The advantage of this
274 approach is that only one point per circle need be identified for plane fitting.
275 UCS can be predicted from fitted c' , ϕ^* and ϕ^B values via

$$\text{UCS} = 2 \left(\frac{c' + \psi \tan \phi^B}{1 - \tan \phi^*} \right) \quad (11)$$

276 as derived in the Appendix. Note that $\phi^* \equiv \phi'$ and $\phi^B \equiv \phi^b$ in function for the
277 failure envelope defined using circle maxima. $\phi^* \neq \phi'$ and $\phi^B \neq \phi^b$, however they
278 are similar for most soils (Powrie, 2008).

279 (Insert Figure 10 somewhere near here)

280 To examine the validity of the simplified approach, UCS values for Soils 4-
281 5-1 and 2-7-1 were re-predicted using Eqn 11. Measured and predicted values
282 are compared in Figure 11. As for Figure 8, distinctions were made between
283 strengths at suctions above and below the maximum ITS suction. With the
284 exception of one result for Soil 4-5-1, results fall largely between the line of
285 equality and an overprediction of roughly 0.15 MPa. The simplified method
286 is therefore no less accurate, within the confines of available results, than the

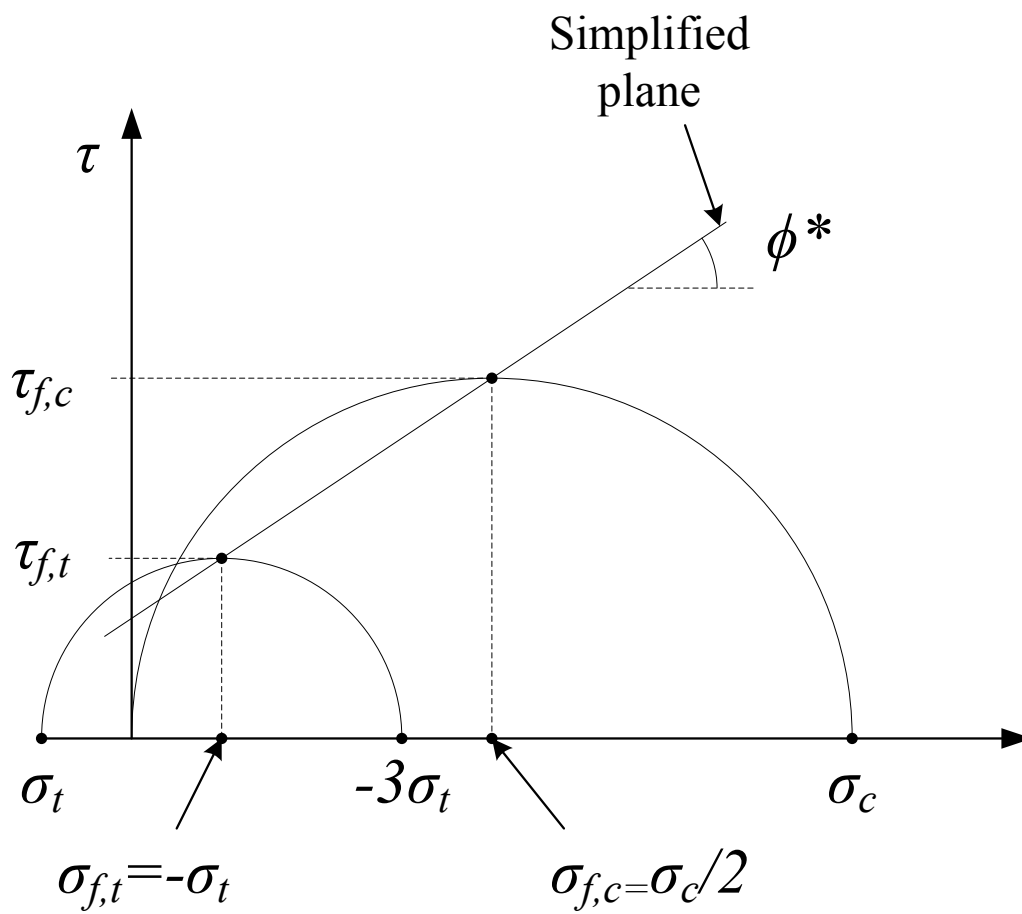


Figure 10: Construction of EMC failure envelope using circle maxima

287 full method. Strength overprediction is not conservative, however the amount is
288 minor and can be accommodated by any reasonable margin of safety.

289 (Insert Figure 11 somewhere near here)

290 *5.2. Plane fitting*

291 Plane-fitting requires powerful computer software, for example MATLAB.
292 That practitioners and laboratories will have access to such software or expertise
293 in its use is unlikely. The fitting process can be significantly simplified by only
294 testing specimens at the plane ‘corners’, i.e. performing UCS and ITS tests at
295 the minimum and maximum anticipated suction conditions. That this is valid
296 was demonstrated by the good agreement for predictions above the ITS suction
297 limit in Figure 8. ϕ^* , ϕ^B and c' calculations using this simplified method are
298 derived in the Appendix. UCS can then be calculated using Eqn 11 as before.

299 *5.3. Testing equipment and revised experimental procedure*

300 Environmental chambers are large, expensive pieces of equipment and there-
301 fore uncommon in most laboratories. An inexpensive alternative is to use satu-
302 rated salt solutions to equilibrate specimens to target suction values. Potential
303 solutions and corresponding suction values are given in Table 5 (Hall and Allinson,
304 2009). Using this technique, a sealable container is partially filled with the salt
305 solution and the specimen suspended above it until it reaches constant mass.
306 Furthermore, the ITS ‘discs’ used here are not commonly encountered in prac-
307 tice. Cylinders of the same dimensions used for UCS testing can be substituted
308 for the discs; σ_t is given by Eqn 2 as before.

309 Based on these simplifications, an experimental procedure readily accessible
310 and relevant to practitioners can be outlined:

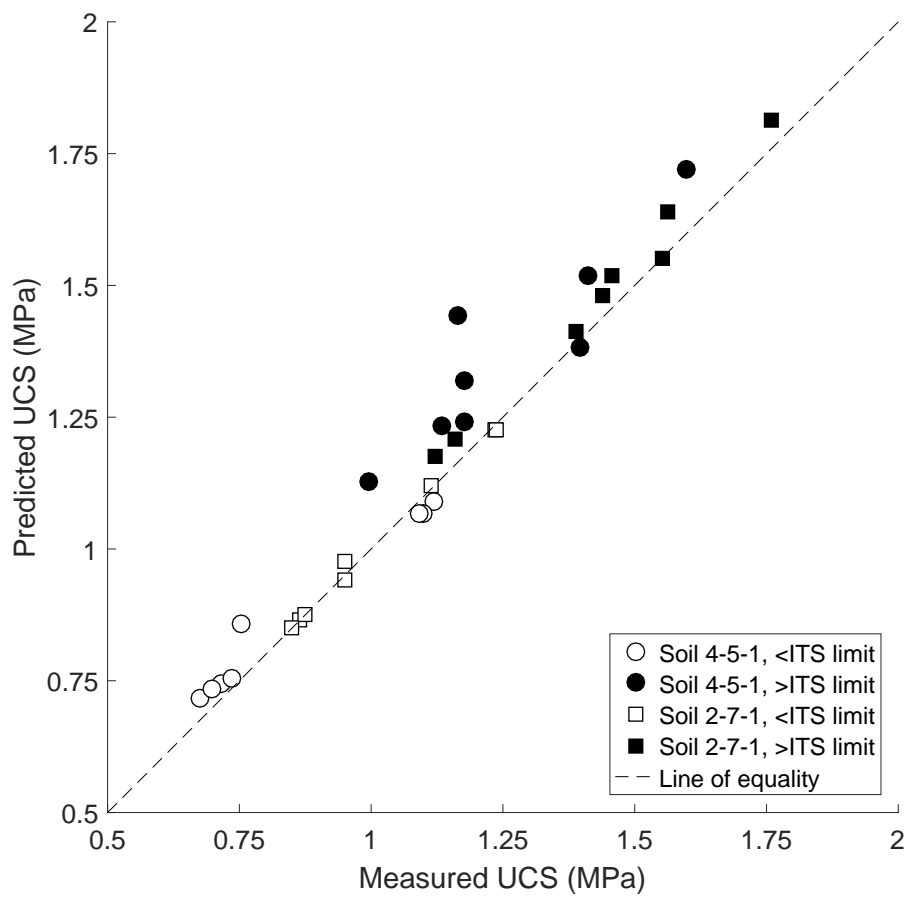


Figure 11: Comparison of measured and predicted UCS values found using the simplified EMC method

Table 5: Saturated salt solutions, associated RH and equivalent suction values for specimen suction equilibration (Hall and Allinson, 2009)

Salt solution	RH at 23°C	Suction (MPa)
Magnesium chloride	32.9±0.2	203.2
Potassium chloride	43.2±0.4	153.4
Magnesium nitrate	53.5±0.2	114.3
Sodium bromide	58.2±0.4	98.9
Sodium chloride	75.4±0.1	51.6
Potassium nitrate	94.0±0.6	11.3

- 311 1. Determine optimum compaction conditions for the proposed soil using stan-
312 dard testing methods (e.g. AS1289, BS1377 etc.).
- 313 2. Obtain ambient site RH and T data (e.g. from government meteorological
314 agencies) and calculate likely minimum and maximum suction conditions
315 using Eqn 1.
- 316 3. Identify suitable salt solutions for this suction range (Table 5).
- 317 4. Manufacture three specimens (at the optimum compaction conditions) per
318 suction condition for UCS and ITS testing.
- 319 5. Seal specimens in containers and periodically check mass until it becomes
320 constant.
- 321 6. Test specimens for UCS or ITS using methods described in this paper. UCS
322 or ITS is the average of the three specimen strengths.
- 323 7. Calculate c' , ϕ^* and ϕ^B using simplified EMC method (Eqns 20 to 28).
- 324 8. Use EMC parameters to predict strengths for suction range of interest
325 (Eqn 11).

326 5.4. Implementation of simplified testing programme

327 To test its practicality, the simplified testing programme outlined above was
328 implemented at an RE construction facility (Watershed Materials) in California,

329 USA. $\varnothing 150 \times 300$ mm UCS and ITS specimens were manufactured from a local
330 rock aggregate, modified with 25% “C-Red” clay by mass (LL 24.1%, PL 16.2%,
331 predominantly kaolinitic with a high iron content). Cylindrical specimens were
332 selected for consistency with preferred industry practice. The final material’s par-
333 ticle grading curve is shown in Figure 12. OWC (7.8%) and $\rho_{d,max}$ (2100kg/m³)
334 were determined following ASTM-D1557. Specimens were equilibrated at high
335 and low humidities (93% and 34%) at 20°C, equivalent to 9.81 and 145.9 MPa
336 suction respectively, using the above techniques, and tested in either compres-
337 sion or tension on reaching constant mass. Three specimens were prepared per
338 condition (12 in total).

339 (Insert Figure 12 somewhere near here)

340 To test the procedure’s ability to successfully predict strength across the suc-
341 tion range, a failure plane was fitted to ITS results and UCS results at low suction
342 only (i.e. using only three of the four ‘corners’ to define the plane). UCS and
343 ITS results and the best-fitted failure plane to the selected Mohr’s circles (using
344 circle maxima) are shown in Figure 13. EMC parameters are given in Table 6;
345 c' , ϕ^* and ϕ^B values were similar to equivalent parameter values found for Soils
346 4-5-1 and 2-7-1, likely due to the similar soil textures, densities and suction range.
347 Agreement between the two indicated that the simplified procedure was able to
348 capture reliable and representative EMC parameters; in the absence of a SWRC,
349 however, ϕ^B predictions using Eqn 9 could not be made. Strengths predicted
350 from the restricted dataset are compared to those found by fitting a plane to all
351 available data in Figure 14. As expected, excellent agreement was found between
352 predicted and measured values using the full dataset due to the fitting nature of
353 the procedure. Using the restricted dataset, predicted strengths were, at most,
354 0.1MPa higher than measured values, i.e. within the anticipated accuracy found

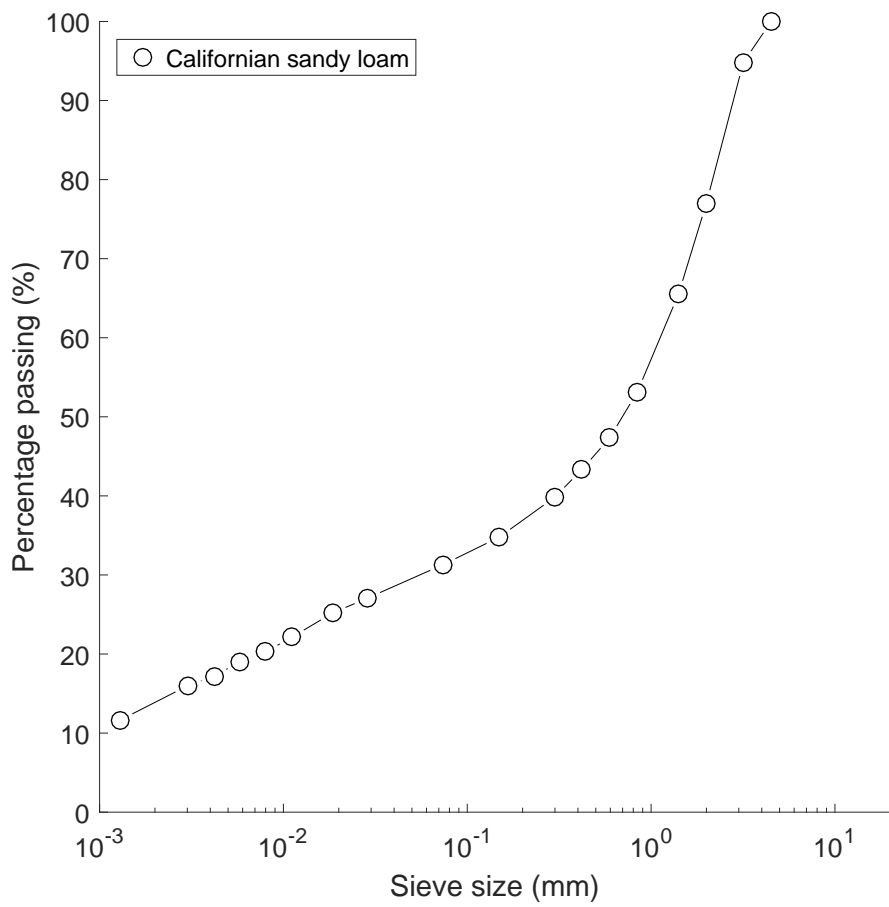


Figure 12: Particle grading curve for modified Californian sandy loam

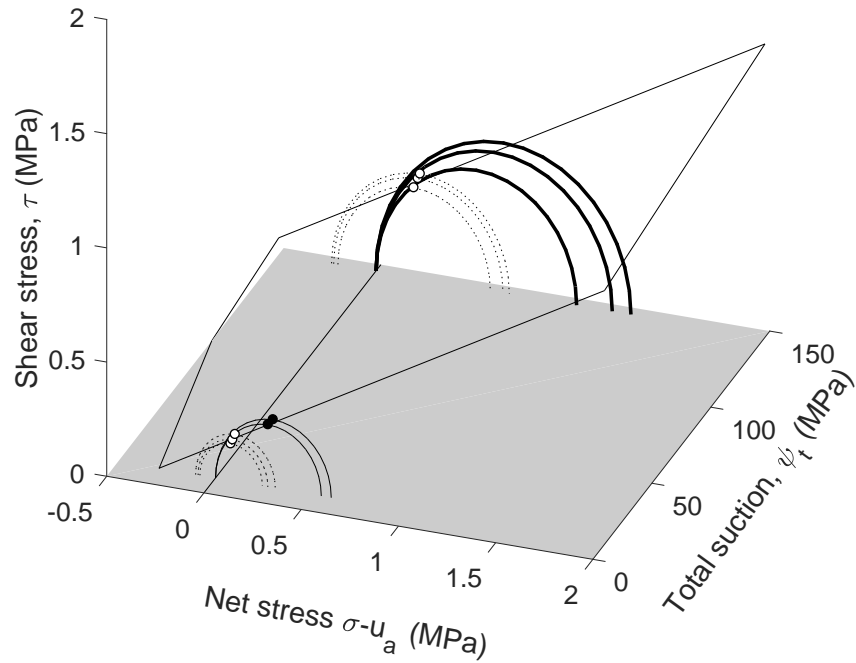


Figure 13: Planar EMC failure envelope for the Californian sandy loam. - UCS results; - - ITS results. Markers denote points on the circles used for plane fitting. Bold circles were omitted from plane-fitting for comparison to predicted values. Note that one UCS specimen at low suction was damaged prior to testing and so was not included

355 for the full procedure.

356 (Insert Figure 13 somewhere near here)

357 (Insert Figure 14 somewhere near here)

358 6. Conclusions

359 Strength uncertainty is a critical obstacle preventing RE's use in wider engi-
 360 neering and construction practice. Recent research has demonstrated that suction

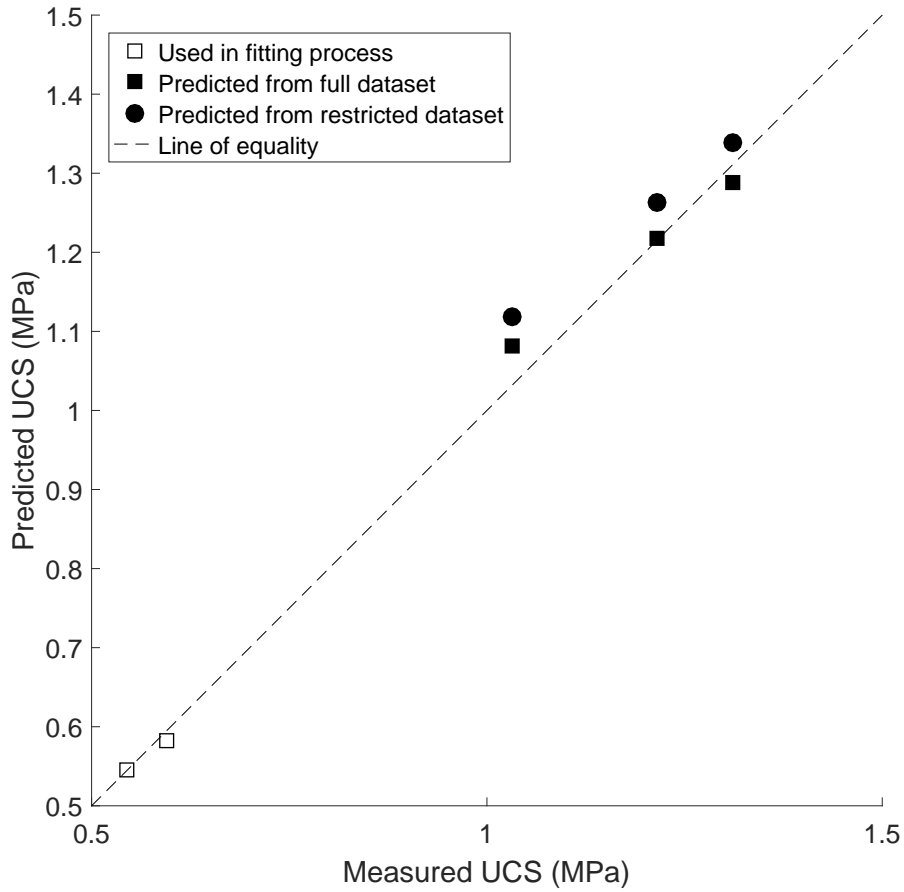


Figure 14: Comparison of measured and predicted UCS values for the Californian sandy loam found using the simplified EMC method and a restricted or complete dataset

Table 6: EMC parameters derived for the Californian sandy loam using the restricted and full dataset

Soil	c' (kPa)	ϕ^* ($^\circ$)	ϕ^B ($^\circ$)	Suction range (MPa)
Restricted dataset	112.7	30.0	0.075	9.81–145.9
Full dataset	128.6	25.9	0.073	9.81–145.9

361 is a key element controlling strength development in these materials. Developing
362 a technique to reliably and realistically characterise strengths is key to improving
363 confidence in RE design, construction and conservation programmes.

364 This paper presents suction-controlled UCS and ITS results for soils repre-
365 sentative of the range and mineralogies likely to be used for RE construction.
366 Strengths were found to almost double between the lowest and highest suctions
367 for both soils. The EMC method was introduced to describe and predict strength
368 changes with suction. Construction of the failure envelope was discussed and the
369 use of a planar failure envelope in the residual suction range justified. Using
370 this technique, good agreement (± 0.15 MPa) was found between measured and
371 predicted strengths for both tested soils across the entire suction range. Good
372 agreement was also found when the technique was applied to literature data of
373 varying suction ranges. Simplifications to the failure plane selection, fitting and
374 experimental techniques were identified to adapt the developed technique to suit
375 RE practice. The simplified plane selection and fitting techniques were tested on
376 UCS and ITS data with no demonstrable loss in accuracy. Finally, the simplified
377 experimental procedure was used to investigate strengths of a compacted Cali-
378 fornian sandy loam tested at an existing RE construction facility. The simplified
379 technique successfully predicted strengths over the entire suction range with the
380 same accuracy as found for the full method.

381 **Acknowledgements**

382 The first author was supported by a studentship awarded by the School of
383 Engineering and Computing Sciences, Durham University whilst this research
384 was undertaken and is now supported by ARC Linkage Grant LP140100375.

385 **References**

- 386 ASTM, 2010. ASTM D5298-10. Standard test method for measurement of soil potential (suction)
387 using filter paper.
- 388 Beckett, C. T. S., Augarde, C., 2012. The effect of relative humidity and temperature on the
389 unconfined compressive strength of rammed earth. In: Mancuso, C., Jommi, C., D'Onza,
390 F. (Eds.), *Unsaturated Soils: Research and Applications*. Second European Conference on
391 *Unsaturated Soils*. Springer Berlin Heidelberg, pp. 287–292.
- 392 Beckett, C. T. S., Smith, J. C., Ciancio, D., Augarde, C. E., 2015. Tensile strengths of flocculated
393 compacted unsaturated soils. *Géotechnique Letters* 5 (4), 254–260.
- 394 BSI, 1990. BS 1377:1990. Methods of testing for soils for civil engineering purposes.
- 395 Bui, Q.-B., Morel, J.-C., Hans, S., Walker, P., 2014. Effect of moisture content on the mechanical
396 characteristics of rammed earth. *Construction and Building Materials* 54, 163–169.
- 397 Ciancio, D., Beckett, C. T. S., Carraro, J., 2014. Optimum lime content identification for lime-
398 stabilised rammed earth. *Construction and Building Materials* 53, 59–65.
- 399 Fredlund, D., Rahardjo, H., 1993. *Soil mechanics for unsaturated soils*. John Wiley & Sons Inc.,
400 New York (USA).
- 401 Fredlund, D. G., Morgenstern, N. R., 1977. Stress state variables for unsaturated soils. *Journal*
402 *of the Geotechnical Engineering Division* 107 (GT5), 447–466.
- 403 Fredlund, D. G., Rahardjo, H., Gan, J. K.-M., 1–4 December 1987. Non-linearity of strength
404 envelope for unsaturated soils. In: *Proceedings of the 6th International Conference on Ex-*
405 *pansive Soils*. New Delhi, India, pp. 49–54.
- 406 Fredlund, D. G., Xing, A., 1994. Equations for the soil-water characteristic curve. *Canadian*
407 *Geotechnical Journal* 31 (4), 521–532.
- 408 Fredlund, D. G., Xing, A., Fredlund, M. D., Barbour, S. L., 1996. The relationship of the
409 unsaturated soil shear strength functions to the soil-water characteristic curve. *Canadian*
410 *Geotechnical Journal* 32, 440–448.
- 411 Frydman, S., 1964. The applicability of the Brazilian (indirect tension) test to soils. *Australian*
412 *Journal of Applied Science* 15 (4), 335–343.
- 413 Gan, J. K. M., Fredlund, D. G., Rahardjo, H., 1988. Determination of the shear strength
414 parameters of an unsaturated soil using the direct shear test. *Can. Geotech. J.* 25 (3), 500–
415 510.

416 Gerard, P., Mahdad, M., McCormack, A. R., François, B., 2015. A unified failure criterion for
417 unstabilized rammed earth materials upon varying relative humidity conditions. *Construction*
418 *and Building Materials* 95, 437–447.

419 Hall, M., Allinson, D., 2009. Analysis of the hygrothermal functional properties of stabilised
420 rammed earth materials. *Building and Environment* 44 (9), 1935–1942.

421 Hall, M., Djerbib, Y., 2004. Moisture ingress in rammed earth: Part 1 - the effect of soil particle-
422 size distribution on the rate of capillary suction. *Construction and Building Materials* 18 (4),
423 269–280.

424 Hamblin, A. P., 1981. Filter paper method for routine measurement of field water potential.
425 *Journal of Hydrology* 53 (3/4), 355–360.

426 Houben, H., Guillaud, H., 1996. *Earth construction - a comprehensive guide.*, Second Edition.
427 Intermediate Technology Publications, London (UK).

428 Jaquin, P. A., Augarde, C. E., Gallipoli, D., Toll, D. G., 2009. The strength of unstabilised
429 rammed earth materials. *Géotechnique* 59 (5), 487–490.

430 Khalili, N., Khabbaz, M. H., 1998. A unique relationship for χ for the determination of the
431 shear strength of unsaturated soils. *Géotechnique* 48 (6), 681–687.

432 Li, D., Wong, L. N. Y., 2013. The Brazilian disc test for rock mechanics applications: Review
433 and new insights. *Rock Mechanics and Rock Engineering* 46 (2), 269–287.

434 McGregor, F., Heath, A., Maskell, D., Fabbri, A., Morel, J.-C., 2015. A review on the buffering
435 capacity of earth building materials. *Construction Materials*.

436 NZS, 1998. NZS 4297:1998. Engineering design of earth buildings.

437 Panayiotopoulos, K. P., 1996. The effect of matric suction on stress-strain relation and strength
438 of three alfisols. *Soil and Tillage Research* 39 (1-2), 45–59.

439 Powrie, W., 2008. *Soil Mechanics: Concepts and Applications*, 2nd Edition. Spon Press.

440 Standards Australia, 2003. AS1289.5.2.1.-2003. Methods of testing soils for engineering purposes.
441 Method 5.2.1: Soil compaction and density tests Determination of the dry density/moisture
442 content relation of a soil using modified compactive effort.

443 Vanapalli, S. K., Fredlund, D. G., Pufahl, D. E., Clifton, A. W., 1996. Model for the prediction
444 of shear strength with respect to soil suction. *Can. Geotech. J.* 33 (3), 379–392.

445 Walker, P., Standards Australia, 2002. Hb 195: The Australian earth building handbook.

446 **Appendix**

447 *Full EMC strength prediction*

448 Derivation of Eqn 10 using Figure 15 for the full EMC method:

$$\tau_{f,pred} = c' + \sigma_{f,pred} \tan \phi' + \psi \tan \phi^b = \frac{\sigma_{c,pred}}{2} \cos \phi' \quad (12)$$

$$\sigma_{f,pred} = \frac{\sigma_{c,pred}}{2} (1 - \sin \phi') \quad (13)$$

449 Substitute Eqn 13 into 12 to find UCS, $\sigma_{c,pred}$:

$$\frac{\sigma_{c,pred}}{2} \cos \phi' = c' + \left(\frac{\sigma_{c,pred}}{2} (1 - \sin \phi') \right) \tan \phi' + \psi \tan \phi^b \quad (14)$$

$$\sigma_{c,pred} = 2 \left(\frac{c' + \psi \tan \phi^b}{\cos \phi' - (1 - \sin \phi') \tan \phi'} \right) \quad (15)$$

450 (Insert Figure 15 somewhere near here)

451 *EMC strength prediction using circle maxima*

452 Derivation of Eqn 11 using Figure 10 for the EMC method using circle max-
453 ima:

$$\tau_{f,pred} = c' + \sigma_{f,pred} \tan \phi^* + \psi \tan \phi^B = \frac{\sigma_{c,pred}}{2} \quad (16)$$

$$\sigma_{f,pred} = \frac{\sigma_{c,pred}}{2} \quad (17)$$

454 Substitute Eqn 17 into 16 to find UCS, $\sigma_{c,pred}$:

$$\frac{\sigma_{c,pred}}{2} = c' + \left(\frac{\sigma_{c,pred}}{2} \right) \tan \phi^* + \psi \tan \phi^B \quad (18)$$

$$\sigma_{c,pred} = 2 \left(\frac{c' + \psi \tan \phi^B}{1 - \tan \phi^*} \right) \quad (19)$$

455 (Insert Figure 16 somewhere near here)

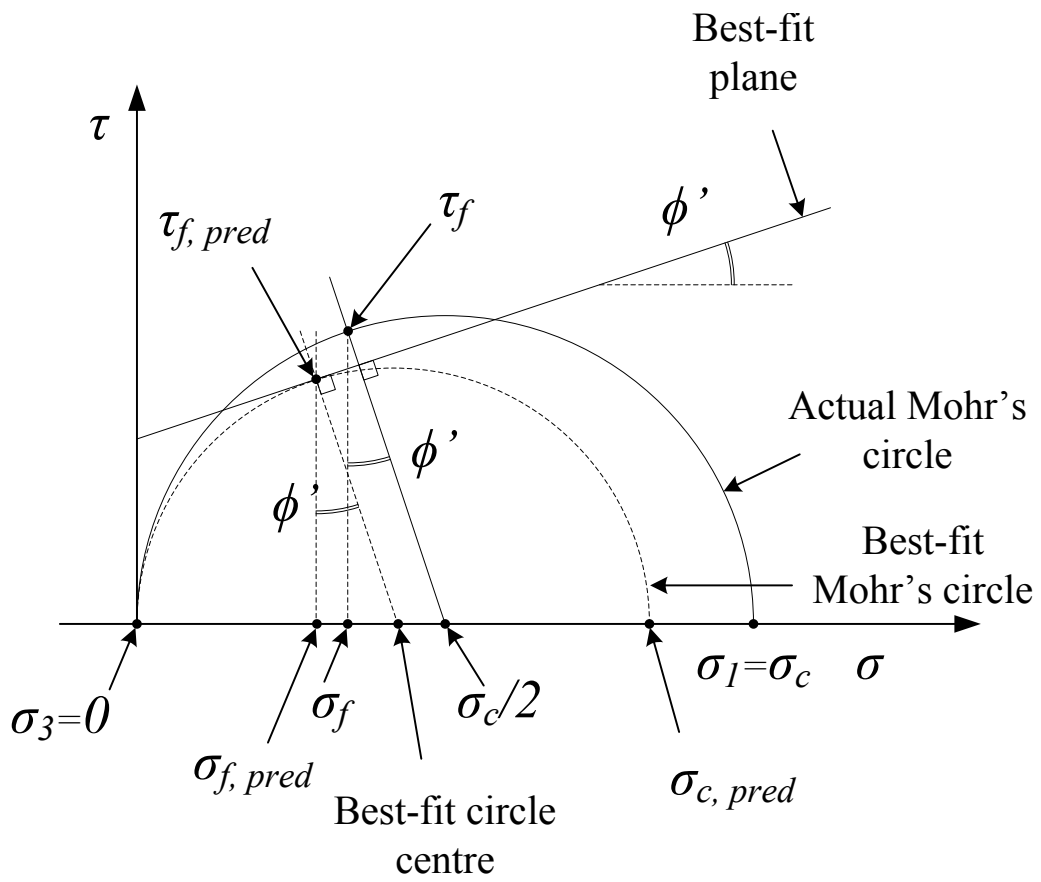


Figure 15: UCS calculation using full EMC method

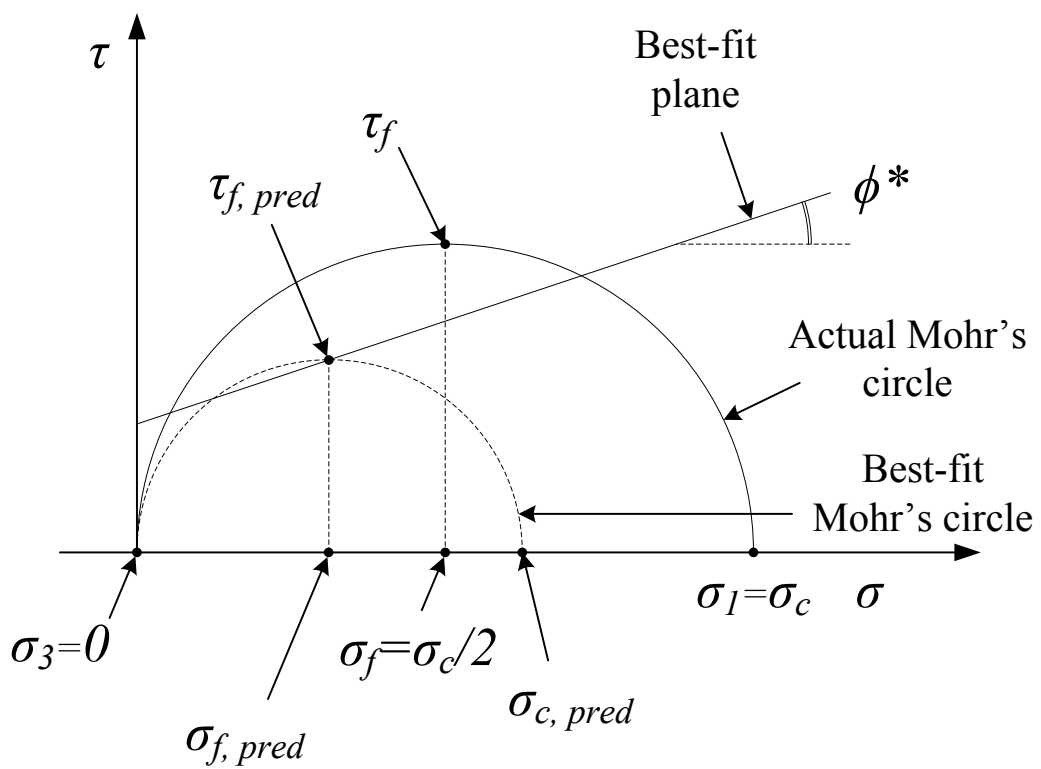


Figure 16: UCS calculation using full EMC method and circle maxima

456 *Simplified EMC strength prediction*

457 EMC parameter calculation using measured UCS and ITS values at plane
458 corner points, using relationships shown in Figure 10:

$$\tan \phi_1^* = \frac{\sigma_{c1} + 4\sigma_{t1}}{\sigma_{c1} + 2\sigma_{t1}} \quad (20)$$

$$\tan \phi_2^* = \frac{\sigma_{c2} + 4\sigma_{t2}}{\sigma_{c2} + 2\sigma_{t2}} \quad (21)$$

$$\tan \phi^* = \frac{\tan \phi_1^* + \tan \phi_2^*}{2} \quad (22)$$

$$\tan \phi_c^B = \frac{\sigma_{c2} - \sigma_{c1}}{2(\psi_2 - \psi_1)} \quad (23)$$

$$\tan \phi_t^B = \frac{2(\sigma_{t1} - \sigma_{t2})}{\psi_2 - \psi_1} \quad (24)$$

$$\tan \phi^B = \frac{\tan \phi_c^B + \tan \phi_t^B}{2} \quad (25)$$

459 where σ_c and σ_t are measured UCS and ITS values, subscripts t and c stand for
460 tension and compression and subscripts 1 and 2 indicate the lower and upper
461 suction values respectively. c' can be solved by rearranging Eqn 11:

$$c'_1 = \frac{\sigma_c(1 - \tan \phi^*)}{2} - \psi \tan \phi^B \quad (\text{at } \psi_1) \quad (26)$$

$$c'_2 = \frac{\sigma_c(1 - \tan \phi^*)}{2} - \psi \tan \phi^B \quad (\text{at } \psi_2) \quad (27)$$

$$c' = \frac{c'_1 + c'_2}{2} \quad (28)$$

462 Note that σ_t is negative in Eqns 20 to 28.